Main Manuscript for

Temporal orchestration of transcriptional and epigenomic programming underlying maternal embryonic diapause in a cricket model

Kosuke Kataoka[1,2*†], Yuta Shimizu[3†], Ryuto Sanno[4], Yuichi Koshiishi[5], Ken Naito[6], Kei Yura[7,8], Toru Asahi[2,4,8], Shin G. Goto[3*]

1. Division of Biotechnology and Life Science, Institute of Engineering, Tokyo University of Agriculture and Technology, 2-24-16 Naka-cho, Koganei-shi, Tokyo 184-8588, Japan.
2. Comprehensive Research Organization, Waseda University, 2-2 Wakamatsu-cho, Shinjuku-ku, Tokyo 162-8480, Japan.
3. Graduate School of Science, Osaka Metropolitan University, 3-3-138 Sugimoto, Sumiyoshi-ku, Osaka 558-8585, Japan.
4. Graduate School of Advanced Science and Engineering, Waseda University, 2-2 Wakamatsu-cho, Shinjuku-ku, Tokyo 162-8480, Japan.
5. Genome Research Center, NODAI Research Institute, Tokyo University of Agriculture, 1-1-1 Sakuragaoka, Setagaya-ku, Tokyo 156-8502, Japan.
6. Research Center of Genetic Resources, National Agriculture and Food Research Organization, 2-1-2 Kannondai, Tsukuba-shi, Ibaraki 305-8602, Japan.
7. Graduate School of Humanities and Sciences, Ochanomizu University, 2-1-1 Otsuka, Bunkyo-ku, Tokyo 112-8610, Japan.
8. Department of Life Science and Medical Bioscience, Waseda University, 513 Waseda Tsurumaki-cho, Shinjuku-ku, Tokyo 162-0041, Japan.

† These authors equally contributed to this work.

* Kosuke Kataoka: kataokak@go.tuat.ac.jp
* Shin G. Goto: shingoto@omu.ac.jp

Author Contributions: K.K., Y. S., and S.G.G. designed research; K.K., Y.S., R.S., Y.K., K.N., K.Y., and T.A. performed research; K.K. analyzed data; and K.K., Y.S., and S.G.G. wrote the paper.

Competing Interest Statement: The authors have no competing interests to disclose.

Classification: Biological Sciences (Developmental Biology)

Keywords: embryonic diapause, maternal effect, transcriptome dynamics, metabolic regulation, *Dianemobius nigrofasciatus*

Abstract

Facultative diapause, a programmed developmental arrest, enables organisms to survive adverse environmental conditions, representing environmentally induced phenotypic plasticity. The band-legged ground cricket *Dianemobius nigrofasciatus* provides a unique model for studying diapause mechanisms, exhibiting maternal diapause induction where short-day exposure of mothers triggers embryonic diapause in offspring at the cellular blastoderm stage, the earliest diapause entry point among insects. Here, we investigated how maternally transmitted environmental signals regulate embryonic development at the molecular level. We assembled a high-quality genome (1.45 Gbp) and performed time-series transcriptomic analyses of diapause and non-diapause eggs from 12 to 72 hours post-oviposition (hpo). Despite morphological similarity at 12-24 hpo, diapause-destined eggs showed specific upregulation of ATP-dependent chromatin remodeling genes, particularly Brahma complex core subunits, at 24 hpo. ATAC-seq analysis at 24 hpo revealed reduced chromatin accessibility near neural and cell cycle-related genes in these eggs. Time-series clustering identified a temporal shift, where RNA processing genes peaked at 24 hpo in diapause-destined eggs versus 40 hpo in non-diapause eggs that undergo direct development, suggesting temporal reorganization allows completion of transcriptional processing before developmental arrest. After diapause initiation (56-72 hpo), while non-diapause eggs upregulated neural differentiation and proliferation genes, diapause eggs showed enhanced expression of amino acid metabolism and gluconeogenesis genes, indicating metabolic regulation for long-term survival. Our findings reveal diapause as an actively regulated developmental state involving coordinated epigenetic, transcriptional, and metabolic remodeling. This cricket model provides insights into how maternal environmental signals guide offspring development through integrated molecular mechanisms, with implications for understanding phenotypic plasticity.

Significance Statement

Organisms have evolved sophisticated mechanisms to integrate environmental signals for developmental control, including diapause, a programmed developmental arrest that enables survival during adverse conditions. Maternal effects, where mothers transmit environmental information to influence offspring developmental fate, represent a particularly powerful strategy for controlling diapause induction across diverse taxa. Using the cricket *Dianemobius nigrofasciatus*, we reveal the molecular orchestration underlying maternal diapause induction. Our integrated multi-omics approach demonstrates that diapause preparation involves precocious activation of chromatin remodeling and RNA processing machinery, followed by comprehensive metabolic restructuring. These findings establish this cricket as an emerging model for diapause research, and reveal coordinated molecular mechanisms that provide a framework for understanding transgenerational environmental adaptation and maternal programming of developmental dormancy across diverse taxa.

Main Text

Introduction

Across the tree of life, organisms have evolved remarkable strategies to survive temporarily hostile environments through dormancy, a physiological state characterized by dramatically reduced metabolic activity that enhances survival during adverse conditions (1, 2). Among the most widespread environmental challenges is seasonality, which poses significant physiological demands on organisms inhabiting temperate regions. To survive periods unsuitable for growth and reproduction, diverse taxa have independently evolved dormancy strategies: hibernation and torpor in mammals and birds, as well as embryonic developmental arrest in vertebrates and developmental pauses in numerous invertebrates, notably insects (3).

Among these strategies, diapause emerges as a programmed form of dormancy employed by many insect species in anticipation of seasonal stressors. Diapause can occur at any developmental stage—egg, larva, pupa, or adult—depending on the species-specific life cycle strategy (4). A number of common physiological events are associated with diapause, including metabolic suppression and developmental arrest (5), enhanced resistance to cold and desiccation (6, 7), and accumulation of energy reserves (8).

In many species, individuals enter diapause upon receiving a token stimulus. However, a particularly intriguing mechanism involves maternal influence, whereby the mother receives environmental signals and transfers this information to her progeny. This transgenerational effect is referred to as the maternal effect (9). Maternal diapause induction is particularly valuable for embryonic diapause, a situation in which an individual has limited access to or time to independently evaluate seasonal conditions. This transgenerational adaptation has been well-documented across diverse taxa, including mites (10), crickets (11–13), rice leaf bug (14), flies (15), mosquitoes (16), and parasitic wasps (17, 18).

Despite the growing interest in maternal diapause induction, the underlying molecular mechanisms remain poorly understood. Recent omics studies have highlighted the importance of alterations in endocrine signaling, cell proliferation, metabolism, and energy production in maternal diapause induction (19, 20); however, these investigations have not comprehensively addressed how maternal influences impact specific molecular pathways initiating diapause, due to limited sampling periods. A comprehensive understanding of the molecular processes through which maternal environmental signals redirect the developmental trajectory towards diapause requires investigation of multiple time points throughout early development.

Dianemobius nigrofasciatus, the band-legged ground cricket, serves as a prominent model for investigating the maternal effect on embryonic diapause (Fig. 1a and 1b) (13, 21). Adult females reared under long-day conditions produce eggs that develop directly into nymphs without undergoing diapause (hereafter called long-day eggs), whereas those exposed to short-day conditions lay diapause-destined eggs (hereafter called short-day eggs) (Fig. 1b) (12, 13). A previous morphological study (22) established that long- and short-day eggs remain visually indistinguishable until 56 hours post-oviposition (hpo). During the first 40 hpo, energids (early embryonic cells) proliferate and migrate to the egg surface in both egg types. Subsequently, between 40 and 56 hpo, both types of eggs undergo cellular blastoderm formation. However, by 72 hpo, a clear morphological divergence emerges: long-day eggs proceed to form a germ band

at the posterior pole, while short-day eggs arrest at the cellular blastoderm stage without germ band formation. Although the involvement of suppressed cell cycle regulators, small silencing RNAs, and segment patterning genes has been suggested (23), the precise molecular mechanisms underlying maternal diapause induction remain unknown.

In this study, we assembled a high-quality genome of *D. nigrofasciatus* and conducted a comprehensive time-series transcriptomic analyses of long- and short-day eggs to elucidate the molecular events occurring before and after the onset of embryonic diapause. Based on the morphological milestones, we strategically selected timepoints that would capture molecular changes before (12 and 24 hpo), during (40 and 56 hpo), and after (72 hpo) the critical developmental decision point where diapause and non-diapause trajectories diverge. Our findings suggest that this process is orchestrated not by a straightforward developmental switch, but rather by a sophisticated temporal orchestration of molecular programs.

Results

Chromosome-scale genome assembly and gene annotation of *D. nigrofasciatus*

To investigate the molecular mechanisms of maternal diapause induction, we generated a chromosome-scale genome assembly of *D. nigrofasciatus* using short-read, long-read, and Omni-C sequencing technologies. Flow cytometry revealed genome size differences between sexes, with males (1496.9 Mbp) having smaller genomes than females (1612.6 Mbp) (Fig. 1c, SI Appendix, Table S1), consistent with the XO/XX sex determination system in crickets (24). *K*-mer analysis estimated a haploid genome size of 1.24 Gbp, which is smaller than the flow cytometry estimates, likely due to underrepresentation of repetitive sequences in short-read data (SI Appendix, Fig S1, Table S2).

The hybrid assembly strategy integrated 100.84× Illumina, 19.87× Oxford Nanopore, and 78.82× Omni-C coverage (SI Appendix, Table S3), resulting in a 1.45 Gbp assembly across 482 scaffolds with a scaffold N50 of 154 Mbp and minimal contamination (SI Appendix, Fig S2). 87.1% of sequences were anchored into 10 linkage groups (Fig. 1d, SI Appendix, Fig S3, Tables S4 and S5). Coverage analysis of male genomic sequences revealed that LG8 and LG9 constitute the X chromosome (SI Appendix, Fig S4, Table S6).

Assembly quality assessment using BUSCO (Benchmarking Universal Single-Copy Orthologs) (25) demonstrated high completeness, with 90.0% complete single-copy and 6.2% duplicated orthologs for the Arthropoda dataset (n=1,013) (Fig. 1e, SI Appendix, Table S4). When evaluated against the more specific Insecta dataset (n=1,367), the assembly showed even higher completeness with 93.2% single-copy and 3.0% duplicated orthologs (Fig. 1e, SI Appendix, Table S4). Gene annotation using BRAKER3 (26–28), StringTie2 (29), and GeMoMa (30) yielded 20,812 protein-coding genes (SI Appendix, Table S7). Phylogenetic analysis of 334 single-copy orthologs placed *D. nigrofasciatus* within Trigonidiidae, sister to Gryllidae (SI Appendix, Fig. S5),consistent with previous studies (31–33).

This high-quality genome assembly and gene annotation provide crucial resources for elucidating the mechanisms of transgenerational diapause programming.

Gradual molecular divergence in maternal diapause induction

To elucidate the molecular mechanisms underlying maternal diapause induction, we performed comprehensive time-series RNA-seq analysis of both long- and short-day eggs at five

developmental timepoints: 12, 24, 40, 56, and 72 hpo (Fig. 2a). Principal component analysis (PCA) of the transcriptome data revealed intriguing patterns in the temporal dynamics of developmental divergence (Fig. 2b). Given that maternal diapause induction presumably involves signaling from mother to offspring, we initially expected substantial transcriptomic differences even at the earliest timepoint. However, molecular differences between long- and short-day eggs were minimal at 12-24 hpo, despite both egg types having been exposed to different maternal environments. The transcriptomic distance between the two egg types then expanded progressively from 24 to 72 hpo, with the most dramatic separation occurring between 56 and 72 hpo, coinciding with morphological divergence.

Differential expression analysis substantiated these observations, revealing a progressive increase in the number of differentially expressed genes (DEGs) between long- and short-day eggs over time ($|\log_2$ fold change$| > 1$, adjusted p-value < 0.05) (Fig. 2c, left panel, SI Appendix, Table S8). Remarkably, at 12 hpo, merely 31 genes showed differential expression (16 upregulated, 15 downregulated in short-day eggs), far fewer than anticipated for a maternally controlled developmental switch. This number increased modestly to 120 DEGs at 24 hpo, then expanded more substantially to 371 DEGs at 40 hpo, 486 DEGs at 56 hpo, and culminated in 1,994 DEGs at 72 hpo (1,078 upregulated, 916 downregulated in short-day eggs).

Analysis of temporal gene expression changes between consecutive timepoints revealed three distinct developmental phases (Fig. 2c, right panel, SI Appendix, Table S9). The first major transcriptional transition (24-40 hpo) coincided with energid proliferation and migration, showing 3,316 DEGs in long-day eggs and 3,104 DEGs in short-day eggs. Transcriptional activity then decreased during cellular blastoderm formation (40-56 hpo), with 858 and 722 DEGs in long- and short-day eggs, respectively. The final phase (56-72 hpo) showed divergent patterns, particularly in long-day eggs (2,922 DEGs) compared to short-day eggs (2,031 DEGs), reflecting the initiation of germ band formation in long-day eggs while short-day eggs undergo molecular changes associated with diapause (22).

Temporal coordination and divergence of gene expression patterns reveal diapause preparation dynamics

To comprehensively characterize these temporal dynamics and identify genes with similar expression patterns across developmental time, we performed fuzzy c-means clustering using Mfuzz (34) on the time-series transcriptome data. This soft clustering assigns genes to multiple clusters with varying membership degrees. This feature makes it particularly suitable for capturing the continuous nature of developmental processes. Following independent clustering of each dataset (long- and short-day eggs), we identified cluster pairs between the two egg types that showed significant gene overlap using upper-tail hypergeometric tests (Fig. 3a, SI Appendix, Fig. S6 and S7). These overlapping cluster pairs were further classified based on their temporal expression patterns: "homochronic clusters" displayed synchronized expression dynamics between egg types, while "heterochronic clusters" exhibited temporal shifts in peak expression timing, revealing potential differences in developmental timing between the two trajectories (SI Appendix, Fig. S8, Table S10).

To understand which developmental processes remain conserved, we first examined homochronic gene clusters that maintained synchronized expression between egg types. The majority of homochronic cluster pairs exhibited peak expression during the early developmental periods (12-24 hpo), suggesting that fundamental embryonic processes are largely conserved

before the diapause trajectory diverges (SI Appendix, Fig. S9, Table S11). Analysis of these early-peaking homochronic clusters revealed common activation of essential cellular machinery: genes encoding components of clathrin-coated vesicles and membrane trafficking systems showed high initial expression followed by continuous decline, likely reflecting the utilization of maternally deposited vesicular trafficking machinery (Fig. 3b) (35–37). Both egg types also showed coordinated activation of autophagy-related genes, peptidases, and catabolic processes at 12-24 hpo, suggesting a conserved program for recycling maternal components during early embryogenesis (Fig. 3b) (37–40).

In contrast, heterochronic clusters unveiled critical timing differences in key molecular pathways (SI Appendix, Fig. S10, Table S12). Notably, genes involved in RNA processing and spliceosome function exhibited marked temporal advancement in short-day eggs (Fig. 3c). While these genes peaked at 40 hpo in long-day eggs, corresponding to the onset of cellular blastoderm formation, they reached maximum expression already at 24 hpo in short-day eggs. This precocious activation of RNA processing machinery coincides with the upregulation of chromatin remodeling factors, suggesting a coordinated early establishment of the molecular foundation required for developmental arrest.

Early epigenetic remodeling drives diapause preparation

Differentially expressed genes unveiled the molecular mechanisms initiating diapause (SI Appendix, Table S13). At 12 hpo, the sole significantly enriched pathway was glycolysis/gluconeogenesis, showing downregulation in short-day eggs (Fig. 4a). However, by 24 hpo, this initial metabolic shift had expanded into comprehensive molecular programming, with multiple pathways emerging as significantly enriched between egg types. Most strikingly, ATP-dependent chromatin remodeling genes showed specific upregulation in short-day eggs at this timepoint (Fig. 4a). Detailed examination revealed increased expression of core subunits of the Brahma (SWI/SNF) complex, including *Bap111*, *pont*, and *Bap60* (Fig. 4b). The Brahma complex is a critical and conserved regulator of chromatin accessibility and gene expression (41–43), suggesting that epigenetic remodeling may serve as a molecular switch for diapause induction.

To test this hypothesis, we performed ATAC-seq analysis on 24 hpo eggs to assess genome-wide chromatin accessibility. Short-day eggs exhibited reduced chromatin accessibility specifically near genes associated with neural development and cell cycle regulation (SI Appendix, Fig. S11, Table S14 and S15). Notable examples include *Kr-h1*, encoding a juvenile hormone-responsive transcription factor essential for developmental progression (44), and *crol*, an ecdysone-inducible transcription factor that recruits Polycomb group proteins (45, 46). Additionally, chromatin closure was observed at *Tlk* (Tousled-like kinase), which triggers S-phase entry and histone assembly (47), and *Ssrp*, a FACT complex subunit required for transcription initiation (48). Neural signaling genes also showed reduced accessibility, including synaptic components such as *Tollo* (Toll-6) and *nAChRα1*. This selective chromatin closure likely contributes to the developmental arrest characteristic of diapause. The timing of these chromatin changes before morphological divergence suggests that epigenetic remodeling is not a consequence but rather a driver of diapause preparation.

Metabolic regulation and developmental signaling orchestrate diapause preparation

Following the early establishment of epigenetic and transcriptional regulatory programs, a comprehensive metabolic and developmental restructuring emerged as the next major phase of

diapause preparation. While initial changes were subtle, a dramatic transformation unfolded from 40 hpo onwards, intensifying through the morphological divergence point.

The metabolic shift was characterized by coordinated activation of multiple amino acid degradation pathways. By 56-72 hpo, valine, leucine, and isoleucine degradation, tryptophan metabolism, lysine degradation, and beta-alanine metabolism were significantly upregulated in short-day eggs (Fig. 4a). This was accompanied by increased expression of key gluconeogenic enzymes, with phosphoenolpyruvate carboxykinase 1 (*Pepck1*) showing marked upregulation from 40 hpo and pyruvate carboxylase (*PCB*) increasing progressively from 56 hpo onwards (Fig. 4c). Genes encoding malate-aspartate shuttle components (*Got2* and *Mdh1/2*) also showed elevated expression in short-day eggs at 56-72 hpo (SI Appendix, Fig. S12), suggesting enhanced mitochondrial-cytoplasmic metabolite exchange. These enzymes enable the conversion of amino acid-derived carbon skeletons into glucose (8, 49), suggesting a metabolic strategy to maintain energy homeostasis during impending developmental arrest.

Complementing this metabolic regulation, protein homeostasis pathways showed coordinated adjustment. From 56 hpo onwards, coinciding with peak metabolic restructuring, proteasome, protein processing in the endoplasmic reticulum, and spliceosome pathways were significantly suppressed in short-day eggs (Fig. 4a). This comprehensive downregulation of both protein synthesis and degradation machinery effectively pauses the cellular protein economy to preserve resources for extended dormancy.

Concurrent with these metabolic changes, key developmental signaling pathways diverged between diapause and non-diapause trajectories. At 40 hpo, we observed significant downregulation of TGF-beta signaling in short-day eggs (Fig. 4a). As a master regulator of cell proliferation and differentiation (50, 51), suppression of TGF-beta signaling effectively applies molecular brakes on developmental progression, occurring before morphological divergence.

Discussion

Our comprehensive molecular analysis reveals that maternal diapause induction in *D. nigrofasciatus* proceeds through a precisely orchestrated temporal cascade of molecular events (Fig. 4d). Both long- and short-day eggs initially share common early developmental processes, including endocytosis and autophagy for recycling maternal components (12-24 hpo). However, short-day eggs diverge through a distinctive molecular program: early activation of chromatin remodeling machinery and precocious RNA processing (24-40 hpo), followed by progressive metabolic restructuring with upregulation of amino acid catabolism and gluconeogenesis pathways that continues through 72 hpo. In contrast, long-day eggs maintain sustained protein synthesis machinery, RNA processing at normal developmental timing, and active cell cycle progression leading to cellular differentiation. This temporal progression demonstrates that diapause preparation is not a simple developmental arrest but rather an active programming process requiring substantial molecular investment before the morphological divergence point.

The temporal advancement of components of RNA processing in short-day eggs, peaking at 24 hpo versus 40 hpo in long-day eggs, represents a striking example of heterochronic gene expression. This precocious activation likely serves multiple adaptive functions. First, the early investment in RNA processing capacity could enable the preparation of stable mRNA pools that persist throughout the diapause period (52, 53). Second, this enhanced RNA processing

machinery may facilitate rapid transcriptional responses upon receiving diapause-terminating signals, allowing quick resumption of development (52, 53). Third, it may establish diapause-specific alternative splicing programs that generate protein isoforms optimized for dormancy (54). The sustained elevation of these components throughout diapause preparation suggests they play a central role in maintaining the molecular readiness for eventual developmental resumption.

The early upregulation of Brahma complex components at 24 hpo, preceding any morphological changes, suggests that chromatin remodeling serves as the primary molecular switch for diapause induction. This finding aligns with emerging evidence that epigenetic mechanisms underlie phenotypic plasticity across diverse organisms (55–58). The selective reduction in chromatin accessibility at developmental regulators such as *Kr-h1* and *crol* effectively locks cells into a pre-differentiation state, preventing the normal progression of embryonic development (44, 45). This epigenetic regulation occurs during a critical window (within 24 hpo), demonstrating how maternal environmental signals can be translated into stable epigenetic modifications that fundamentally alter offspring developmental trajectory. Intriguingly, this 24-hour window coincides with the period during which temperature pulses can still reverse diapause fate decisions (59), suggesting that chromatin remodeling may define developmental fate plasticity.

The progressive metabolic restructuring observed from 56 hpo onwards reveals a sophisticated survival strategy distinct from simple developmental arrest. The coordinated upregulation of amino acid catabolism pathways and gluconeogenic enzymes indicates a fundamental shift from anabolic growth metabolism to a catabolic maintenance mode. This metabolic flexibility enables short-day eggs to utilize maternally deposited amino acids as an energy source while preserving essential proteins needed for eventual development (8). The timing of these changes, beginning before morphological divergence and intensifying through 72 hpo, indicates that metabolic programming is an integral preparatory component rather than a consequence of arrest. This preemptive metabolic adjustment, coupled with the suppression of protein synthesis and proteasome pathways, creates a molecular economy optimized for long-term survival while maintaining developmental competence (52, 53).

The remarkable plasticity of *D. nigrofasciatus*, which can facultatively switch between diapause and direct development based on maternal photoperiod experience, makes it an unique model for understanding how environmental information is translated into developmental outcomes (13, 21). Our findings illuminate how subtle maternal signals can be progressively amplified into dramatically different developmental outcomes through self-reinforcing molecular cascades that combine epigenetic, transcriptional, and metabolic regulation. This temporal orchestration framework likely extends beyond insects to other organisms that employ maternal programming of developmental dormancy, including delayed implantation in mammals (60, 61), suggesting that coordinated molecular timing represents a fundamental mechanism for transgenerational environmental adaptation across diverse organisms. This cricket model system provides a powerful framework for understanding the universal principles governing how organisms across the tree of life integrate environmental information to orchestrate developmental decisions through conserved molecular mechanisms.

Materials and Methods

Experimental animals and sample collection

Dianemobius nigrofasciatus were maintained under controlled conditions (detailed husbandry in SI Appendix). Eggs were collected at five developmental time points (12, 24, 40, 56, and 72 hpo) from females maintained under diapause-inducing short-day (12 h light: 12 h dark) or non-diapause long-day (16 h light: 8 h dark) photoperiod conditions. Three to five biological replicates were prepared for each condition and time point.

Genome sequencing and assembly

High-quality genomic DNA was extracted from adult males and sequenced using Oxford Nanopore PromethION (30.4 Gbp) and Illumina NovaSeq 6000 (152.7 Gbp) platforms. Chromosome-scale assembly was achieved using Hi-C data (127.1 Gbp) processed with HiRise (62) software. The genome was assembled using MaSuRCA v4.1.0 (63), purged for haplotigs (64), and decontaminated using BlobTools (65) (detailed assembly pipeline in SI Appendix).

RNA-seq analysis

Total RNA was extracted from eggs at each time point and sequenced on Illumina platforms (SI Appendix, Table S16). Transcript quantification was performed using Salmon v1.10.1 (66), and differential expression analysis was conducted using DESeq2 (67) with adjusted p-value < 0.05. Time-series clustering analysis using Mfuzz (34) identified co-expressed gene modules. Functional enrichment was performed using g:Profiler (68) with *Drosophila melanogaster* orthologs (detailed RNA-seq methods in SI Appendix).

ATAC-seq analysis

Chromatin accessibility was profiled using ATAC-seq on eggs collected within 24 hpo (SI Appendix, Table S17). Libraries were prepared using the Active Motif ATAC-seq Kit and sequenced on Illumina NovaSeq 6000. Peaks were called using MACS2 (69), and differential accessibility analysis was performed using edgeR (70) (detailed ATAC-seq protocol in SI Appendix).

Data availability

Raw read data used in this article (RNA-seq, ATAC-seq, Omni-C and WGS) have been submitted at DNA Data Bank of Japan (DDBJ) repository under accession no. PRJDB18895 and are publicly available as of the date of publication. The datasets are available in following link; https://ddbj.nig.ac.jp/resource/bioproject/PRJDB18895. The assembled genome and annotation datasets are available in https://doi.org/10.6084/m9.figshare.29665742.v1.

Acknowledgments

This work was supported by the Cooperative Research Grant of the Genome Research for BioResource (NODAI Genome Research Center, Tokyo University of Agriculture), Cross-ministerial Moonshot Agriculture, Forestry and Fisheries Research and Development Program, "Technologies for Smart Bio-industry and Agriculture" (Bio-oriented Technology Research Advancement Institution, BRAIN) [Grant Number: JPJ009237], JSPS KAKENHI Grant-in-Aid for Scientific Research (C) [Grant Number: 21K05614], and Grant-in-Aid for JSPS Fellows [Grant Number: 21J23478/22KJ2609]. We thank Dr. Tarô Adati (Department of International Agricultural Development, Faculty of International Agriculture and Food Studies, Tokyo University of Agriculture) for his valuable advice and support.

Figures

Figure 1. Life cycle and genomic characterization of the band-legged ground cricket, *Dianemobius nigrofasciatus*. (a) Adult female *D. nigrofasciatus*. **(b)** Annual life cycle diagram in Osaka, Japan, illustrating photoperiod-dependent developmental transitions and diapause regulation. The outer ring represents the developmental stages (egg, nymph, and adult) and the diapause egg state. The inner circle shows seasonal progression with photoperiod-dependent phases: the pink area indicates the period with the longer critical day length, whereas the blue area indicates the period with the shorter critical day length. The first-generation adults emerge in September-October under short-day conditions and produce predominantly diapause-destined eggs that overwinter in the cellular blastoderm stage, whereas the second-generation adults appear in June-August under long-day conditions and produce non-diapause eggs. **(c)** Flow cytometric analysis of brain cells from adult females and males showing genome size estimation. Box plots show the distribution of genome size measurements, with blue numbers indicating mean ± 95% confidence interval for each sex. **(d)** Circos plot depicting genomic features across the ten linkage groups (LG1-10). From outer to inner tracks: gene density (I), repetitive element content (II), and GC content distribution (III). **(e)** BUSCO completeness assessment of the genome assembly and gene annotation against Arthropoda and Insecta databases via the gVolante web server. Colors indicate complete single-copy (solid green), completely duplicated (blue with diagonal stripes), fragmented (yellow crosshatched pattern), and missing (red with black dot pattern) genes.

Figure 2. Transcriptome dynamics during early embryogenesis in long- and short-day eggs of *D. nigrofasciatus*. (a) Schematic representation of developmental progression from 0 to 72 hours post-oviposition (hpo) at 25°C. Adults reared under short-day conditions produce diapause-destined eggs (short-day eggs), while those under long-day conditions produce eggs that undergo direct development (long-day eggs). The morphological features of early embryonic stages were characterized by Tanigawa et al. (2009). In both egg types, nuclei migrate from the yolk mass to the egg surface by 24 hpo. Cellular blastoderm formation occurs between 40-56 hpo in both trajectories. While long-day eggs proceed to form a germ band by 72 hpo, short-day eggs arrest development at the cellular blastoderm stage, maintaining this state throughout the diapause period. **(b)** Three-dimensional principal component analysis of transcriptome profiles across developmental time points. Red and blue marks indicate long- and short-day eggs, respectively. **(c)** *Left panel*: Number of differentially expressed genes (DEGs) between long- and short-day eggs at each developmental timepoint (12, 24, 40, 56, and 72 hpo). DEGs were defined as genes with $|\log_2$ fold change (FC)$| > 1$ and adjusted p-value < 0.05. Green bars with crosshatched pattern indicate genes upregulated in short-day eggs, while yellow bars with diagonal stripes represent genes downregulated in short-day eggs. *Right panels***:** Temporal dynamics of gene expression changes within each egg type, comparing later versus earlier developmental timepoints. For long- (left) and short-day eggs (right), bars show the number of genes upregulated (green with crosshatched pattern) or downregulated (yellow with diagonal stripes) at the later timepoint relative to the earlier timepoint in each comparison ($|\log_2$ FC$| > 1$, adjusted p-value < 0.05).

Figure 3. Comparative analysis of temporal gene expression dynamics between long- and short-day eggs. (a) Heat map showing the significance of gene overlap between temporal expression clusters in long- and short-day eggs across five developmental timepoints (12, 24, 40, 56, and 72 hpo) as derived from an upper-tail hypergeometric test. Gene expression profiles were clustered using the Mfuzz soft clustering algorithm. Numbers on the right and bottom axes represent cluster IDs for long-day and short-day eggs, respectively. Color intensity represents -$\log_{10}$(adjusted *p*-value), with darker red indicating more significant overlap between clusters. Homochronic clusters (highlighted in blue boxes) show conserved temporal expression patterns between the two egg types. Heterochronic clusters (highlighted in green boxes) exhibit shifted temporal dynamics between long- and short-day eggs. **(b1, b2, c1, and c2)** Expression trajectories show representative homochronic **(b)** or heterochronic **(c)** cluster pairs, where color intensity reflects membership scores calculated by Mfuzz (magenta indicating high membership and green indicating low membership). Bar graphs display functional enrichment analysis results using overlapping genes, with terms categorized as GO Biological Process (GO:BP, orange), GO Cellular Component (GO:CC, green), GO Molecular Function (GO:MF, blue), or KEGG pathways (red). For each category, the top five most significantly enriched terms (ranked by adjusted *p*-value) are shown; when fewer than five terms were significant, all enriched terms are displayed. Bar length represents -$\log_{10}$(adjusted *p*-value).

Figure 4. Temporal coordination of biological processes during early embryogenesis in long- and short-day eggs. (a) KEGG pathway enrichment analysis of differentially expressed genes (DEGs) identified between long-day and short-day conditions at each time point (adjusted *p*-value < 0.05). Dot size represents the percentage of DEGs annotated to each pathway, and color intensity indicates the adjusted *p*-value. **(b and c)** Temporal expression patterns (TPM values) of genes involved in chromatin remodeling **(b)** and gluconeogenesis **(c)**. The red frames in (b) highlight the critical periods of expression divergence between long- and short-day eggs. **(d)** Schematic representation of key biological processes and their temporal dynamics from 0 to 72 hpo. Both long- and short-day eggs show similar timing of membrane trafficking processes (endocytosis and autophagy) during early embryogenesis (12-24 hpo). Chromatin remodeling occurs within a specific time window around 24 hpo. Prior to diapause entry at the cellular blastoderm stage, short-day eggs show advanced activation of RNA processing and protein synthesis compared to long-day eggs. During later development (>56 hpo), short-day eggs activate amino acid metabolism and gluconeogenesis pathways, while long-day eggs proceed with neural development and cell cycle progression.

References

1. J. T. Lennon, F. den Hollander, M. Wilke-Berenguer, J. Blath, Principles of seed banks and the emergence of complexity from dormancy. *Nat. Commun.* **12**, 4807 (2021).

2. H. Ö. Özgüldez, A. Bulut-Karslioğlu, Dormancy, quiescence, and diapause: Savings accounts for life. *Annu. Rev. Cell Dev. Biol.* **40**, 25–49 (2024).

3. K. Wilsterman, M. A. Ballinger, C. M. Williams, A unifying, eco-physiological framework for animal dormancy. *Funct. Ecol.* **35**, 11–31 (2021).

4. D. L. Denlinger, *Insect Diapause* (Cambridge University Press, 2022).

5. M. J., C. A. Tauber, S. Masaki, *Seasonal Adaptations of Insects* (Oxford University Press, 1985).

6. J. P. Rinehart, *et al.*, Up-regulation of heat shock proteins is essential for cold survival during insect diapause. *Proc. Natl. Acad. Sci. U. S. A.* **104**, 11130–11137 (2007).

7. J. B. Benoit, Water management by dormant insects: comparisons between dehydration resistance during summer aestivation and winter diapause. *Prog. Mol. Subcell. Biol.* **49**, 209–229 (2010).

8. D. A. Hahn, D. L. Denlinger, Energetics of insect diapause. *Annu. Rev. Entomol.* **56**, 103–121 (2011).

9. T. A. Mousseau, C. W. Fox, The adaptive significance of maternal effects. *Trends Ecol. Evol.* **13**, 403–407 (1998).

10. K. Oku, S. Yano, A. Takafuji, Different maternal effects on diapause induction of tetranychid mites, *Tetranychus urticae* and *T. kanzawai* (Acari: Tetranychidae). *Appl. Entomol. Zool. (Jpn.)* **38**, 267–270 (2003).

11. D. L. Huestis, J. L. Marshall, Interaction between maternal effects and temperature affects diapause occurrence in the cricket *Allonemobius socius*. *Oecologia* **146**, 513–520 (2006).

12. S. Masaki, Climatic adaptation and photoperiodic response in the band-legged ground cricket. *Evolution* **26**, 587–600 (1972).

13. S. Shiga, H. Numata, Seasonal changes in the incidence of embryonic diapause in the band-legged ground cricket, *Dianemobius nigrofasciatus*. *Zool. Sci.* **14**, 1015–1018 (1997).

14. Y. Shintani, Effect of seasonal variation in host-plant quality on the rice leaf bug, *Trigonotylus caelestialium*. *Entomol. Exp. Appl.* **133**, 128–135 (2009).

15. S. Rockey, B. B. Miller, D. Denlinger, A diapause maternal effect in the flesh fly, *Sarcophaga bullata*: Transfer of information from mother to progeny. *Journal of Insect Physiology* **35**, 553–558 (1989).

16. J. Bova, J. Soghigian, S. Paulson, The prediapause stage of *Aedes japonicus japonicus* and the evolution of embryonic diapause in Aedini. *Insects* **10**, 222 (2019).

17. H. A. Schneiderman, J. Horwitz, The induction and termination of facultative diapause in the chalcid wasps *Mormoniella vitripennis* (Walker) and *Tritneptis klugii* (Ratzeburg). *J. Exp. Biol.* **35**, 520–551 (1958).

18. D. S. Saunders, Larval diapause of maternal origin: Induction of diapause in *Nasonia vitripennis* (Walk.) (Hymenoptera: Pteromalidae). *J. Exp. Biol.* **42**, 495–508 (1965).

19. M. F. Poelchau, J. A. Reynolds, C. G. Elsik, D. L. Denlinger, P. A. Armbruster, Deep sequencing reveals complex mechanisms of diapause preparation in the invasive mosquito, *Aedes albopictus*. *Proc. Biol. Sci.* **280**, 20130143 (2013).

20. J. Gong, *et al.*, Early molecular events during onset of diapause in silkworm eggs revealed by transcriptome analysis. *Int. J. Mol. Sci.* **21**, 6180 (2020).

21. T. Kidokoro, S. Masaki, Photoperiodic response in the relation to variable voltinism in the ground cricket, *Pteronemobius fascipes* Walker (Orthoptera: Gryllidae). *Jpn. J. Ecol* **28**, 291–298 (1978).

22. N. Tanigawa, K. Matsumoto, K. Yasuyama, H. Numata, S. Shiga, Early embryonic development and diapause stage in the band-legged ground cricket *Dianemobius nigrofasciatus*. *Dev. Genes Evol.* **219**, 589–596 (2009).

23. Y. Shimizu, T. Tamai, S. G. Goto, Cell cycle regulator, small silencing RNA, and segmentation patterning gene expression in relation to embryonic diapause in the band-legged ground cricket. *Insect Biochem. Mol. Biol.* **102**, 75–83 (2018).

24. H. Blackmon, L. Ross, D. Bachtrog, Sex determination, sex chromosomes, and karyotype evolution in insects. *J. Hered.* **108**, 78–93 (2017).

25. M. Manni, M. R. Berkeley, M. Seppey, F. A. Simão, E. M. Zdobnov, BUSCO update: Novel and streamlined workflows along with broader and deeper phylogenetic coverage for scoring of eukaryotic, prokaryotic, and viral genomes. *Mol. Biol. Evol.* **38**, 4647–4654 (2021).

26. M. Stanke, M. Diekhans, R. Baertsch, D. Haussler, Using native and syntenically mapped cDNA alignments to improve *de novo* gene finding. *Bioinformatics* **24**, 637–644 (2008).

27. M. Stanke, O. Schöffmann, B. Morgenstern, S. Waack, Gene prediction in eukaryotes with a generalized hidden Markov model that uses hints from external sources. *BMC Bioinformatics* **7**, 62 (2006).

28. L. Gabriel, K. J. Hoff, T. Brůna, M. Borodovsky, M. Stanke, TSEBRA: transcript selector for BRAKER. *BMC Bioinformatics* **22**, 566 (2021).

29. S. Kovaka, *et al.*, Transcriptome assembly from long-read RNA-seq alignments with StringTie2. *Genome Biol.* **20**, 278 (2019).

30. J. Keilwagen, F. Hartung, J. Grau, GeMoMa: Homology-based gene prediction utilizing intron position conservation and RNA-seq data. *Methods Mol. Biol.* **1962**, 161–177 (2019).

31. Y. Ito, *et al.*, Chromosome-scale whole genome assembly and annotation of the Jamaican field cricket *Gryllus assimilis*. *Sci. Data* **12**, 826 (2025).

32. K. Murata, *et al.*, Complete mitochondrial genome sequences of two ground crickets, *Dianemobius fascipes nigrofasciatus* and *Polionemobius taprobanensis* (Orthoptera: Grylloidea: Trigonidiidae). *Mitochondrial DNA Part B* **8**, 1311–1315 (2023).

33. R. Sanno, *et al.*, Comparative analysis of mitochondrial genomes in Gryllidea (Insecta: Orthoptera): Implications for adaptive evolution in ant-loving crickets. *Genome Biol. Evol.* **13**, evab222 (2021).

34. L. Kumar, M. E Futschik, Mfuzz: a software package for soft clustering of microarray data. *Bioinformation* **2**, 5–7 (2007).

35. A. Pelissier, J.-P. Chauvin, T. Lecuit, Trafficking through Rab11 endosomes is required for cellularization during *Drosophila* embryogenesis. *Curr. Biol.* **13**, 1848–1857 (2003).

36. T. Lecuit, Junctions and vesicular trafficking during *Drosophila* cellularization. *J. Cell Sci.* **117**, 3427–3433 (2004).

37. F. A. Lefebvre, É. Lécuyer, Flying the RNA nest: *Drosophila* reveals novel insights into the transcriptome dynamics of early development. *J. Dev. Biol.* **6**, 5 (2018).

38. H. Kuhn, R. Sopko, M. Coughlin, N. Perrimon, T. Mitchison, The Atg1-Tor pathway regulates yolk catabolism in *Drosophila* embryos. *Development* **142**, 3869–3878 (2015).

39. M. M. Harrison, M. B. Eisen, Transcriptional activation of the zygotic genome in *Drosophila*. *Curr. Top. Dev. Biol.* **113**, 85–112 (2015).

40. J. D. Laver, A. J. Marsolais, C. A. Smibert, H. D. Lipshitz, Regulation and function of maternal gene products during the maternal-to-zygotic transition in *Drosophila*. *Curr. Top. Dev. Biol.* **113**, 43–84 (2015).

41. J. Shi, *et al.*, *Drosophila* Brahma complex remodels nucleosome organizations in multiple aspects. *Nucleic Acids Res.* **42**, 9730–9739 (2014).

42. A. Möller, F. W. Avila, J. W. Erickson, H. Jäckle, *Drosophila* BAP60 is an essential component of the Brahma complex, required for gene activation and repression. *J. Mol. Biol.* **352**, 329–337 (2005).

43. O. Papoulas, *et al.*, The HMG-domain protein BAP111 is important for the function of the BRM chromatin-remodeling complex *in vivo*. *Proc. Natl. Acad. Sci. U. S. A.* **98**, 5728–5733 (2001).

44. Y. Beck, F. Pecasse, G. Richards, Krüppel-homolog is essential for the coordination of regulatory gene hierarchies in early *Drosophila* development. *Dev. Biol.* **268**, 64–75 (2004).

45. N. Mitchell, N. Cranna, H. Richardson, L. Quinn, The ecdysone-inducible zinc-finger transcription factor Crol regulates Wg transcription and cell cycle progression in *Drosophila*. *Development* **135**, 2707–2716 (2008).

46. M. Erokhin, *et al.*, Crol contributes to PRE-mediated repression and Polycomb group proteins recruitment in *Drosophila*. *Nucleic Acids Res.* **51**, 6087–6100 (2023).

47. P. Carrera, *et al.*, Tousled-like kinase functions with the chromatin assembly pathway regulating nuclear divisions. *Genes Dev.* **17**, 2578–2590 (2003).

48. J. Chen, *et al.*, Piwi regulates the usage of alternative transcription start sites in the *Drosophila* ovary. *Nucleic Acids Res.* **53**, gkae1160 (2025).

49. H. Izadi, Endocrine and enzymatic shifts during insect diapause: a review of regulatory mechanisms. *Front. Physiol.* **16**, 1544198 (2025).

50. X.-S. Zhang, Z.-H. Wang, W.-S. Li, W.-H. Xu, FoxO induces pupal diapause by decreasing TGFβ signaling. *Proc. Natl. Acad. Sci. U. S. A.* **119**, e2210404119 (2022).

51. H.-Y. Li, X.-W. Lin, S.-L. Geng, W.-H. Xu, TGF-β and BMP signals regulate insect diapause through Smad1-POU-TFAM pathway. *Biochim. Biophys. Acta Mol. Cell Res.* **1865**, 1239–1249 (2018).

52. M. Stadler, A. Fire, Conserved translatome remodeling in nematode species executing a shared developmental transition. *PLoS Genet.* **9**, e1003739 (2013).

53. P. R. Clouser, C. L. Riggs, A. L. T. Romney, J. E. Podrabsky, Diapause and anoxia-induced quiescence are unique states in embryos of the annual killifish, *Austrofundulus limnaeus*. *Biomolecules* **15**, 515 (2025).

54. R. A. Steward, P. Pruisscher, K. T. Roberts, C. W. Wheat, Genetic constraints in genes exhibiting splicing plasticity in facultative diapause. *Heredity (Edinb.)* **132**, 142–155 (2024).

55. B. Li, *et al.*, DNA methylation is correlated with gene expression during diapause termination of early embryonic development in the silkworm (*Bombyx mori*). *Int. J. Mol. Sci.* **21**, 671 (2020).

56. Z. Tian, *et al.*, The PBAP chromatin remodeling complex mediates summer diapause via H3K4me3-driven juvenile hormone regulation in *Colaphellus bowringi*. *Proc. Natl. Acad. Sci. U. S. A.* **122**, e2422328122 (2025).

57. P. P. Singh, *et al.*, Evolution of diapause in the African turquoise killifish by remodeling the ancient gene regulatory landscape. *Cell* **187**, 3338–3356 (2024).

58. M. Wrona, *et al.*, The BRAHMA-associated SWI/SNF chromatin remodeling complex controls *Arabidopsis* seed quality and physiology. *Plant Physiol.* **197**, kiae642 (2024).

59. E. Fukumoto, H. Numata, S. Shiga, Effects of temperature of adults and eggs on the induction of embryonic diapause in the band-legged ground cricket, *Dianemobius nigrofasciatus*. *Physiol. Entomol.* **31**, 211–217 (2006).

60. G. E. Ptak, *et al.*, Embryonic diapause is conserved across mammals. *PLoS One* **7**, e33027 (2012).

61. M. R. McGowen, O. Erez, R. Romero, D. E. Wildman, The evolution of embryo implantation. *Int. J. Dev. Biol.* **58**, 155–161 (2014).

62. N. H. Putnam, *et al.*, Chromosome-scale shotgun assembly using an *in vitro* method for long-range linkage. *Genome Res.* **26**, 342–350 (2016).

63. A. V. Zimin, *et al.*, The MaSuRCA genome assembler. *Bioinformatics* **29**, 2669–2677 (2013).

64. M. J. Roach, S. A. Schmidt, A. R. Borneman, Purge Haplotigs: Allelic contig reassignment for third-gen diploid genome assemblies. *BMC Bioinformatics* **19**, 460 (2018).

65. D. R. Laetsch, M. L. Blaxter, BlobTools: Interrogation of genome assemblies. *F1000Res.* **6** (2017).

66. R. Patro, G. Duggal, M. I. Love, R. A. Irizarry, C. Kingsford, Salmon provides fast and bias-aware quantification of transcript expression. *Nat. Methods* **14**, 417–419 (2017).

67. M. I. Love, W. Huber, S. Anders, Moderated estimation of fold change and dispersion for RNA-seq data with DESeq2. *Genome Biol.* **15**, 550 (2014).

68. U. Raudvere, *et al.*, g:Profiler: a web server for functional enrichment analysis and conversions of gene lists (2019 update). *Nucleic Acids Res.* **47**, W191–W198 (2019).

69. Y. Zhang, *et al.*, Model-based analysis of ChIP-Seq (MACS). *Genome Biol.* **9**, R137 (2008).

70. Y. Chen, L. Chen, A. T. L. Lun, P. L. Baldoni, G. K. Smyth, edgeR v4: Powerful differential analysis of sequencing data with expanded functionality and improved support for small counts and larger datasets. *Nucleic Acids Res.* **53**, gkaf018 (2025).

Figure 1

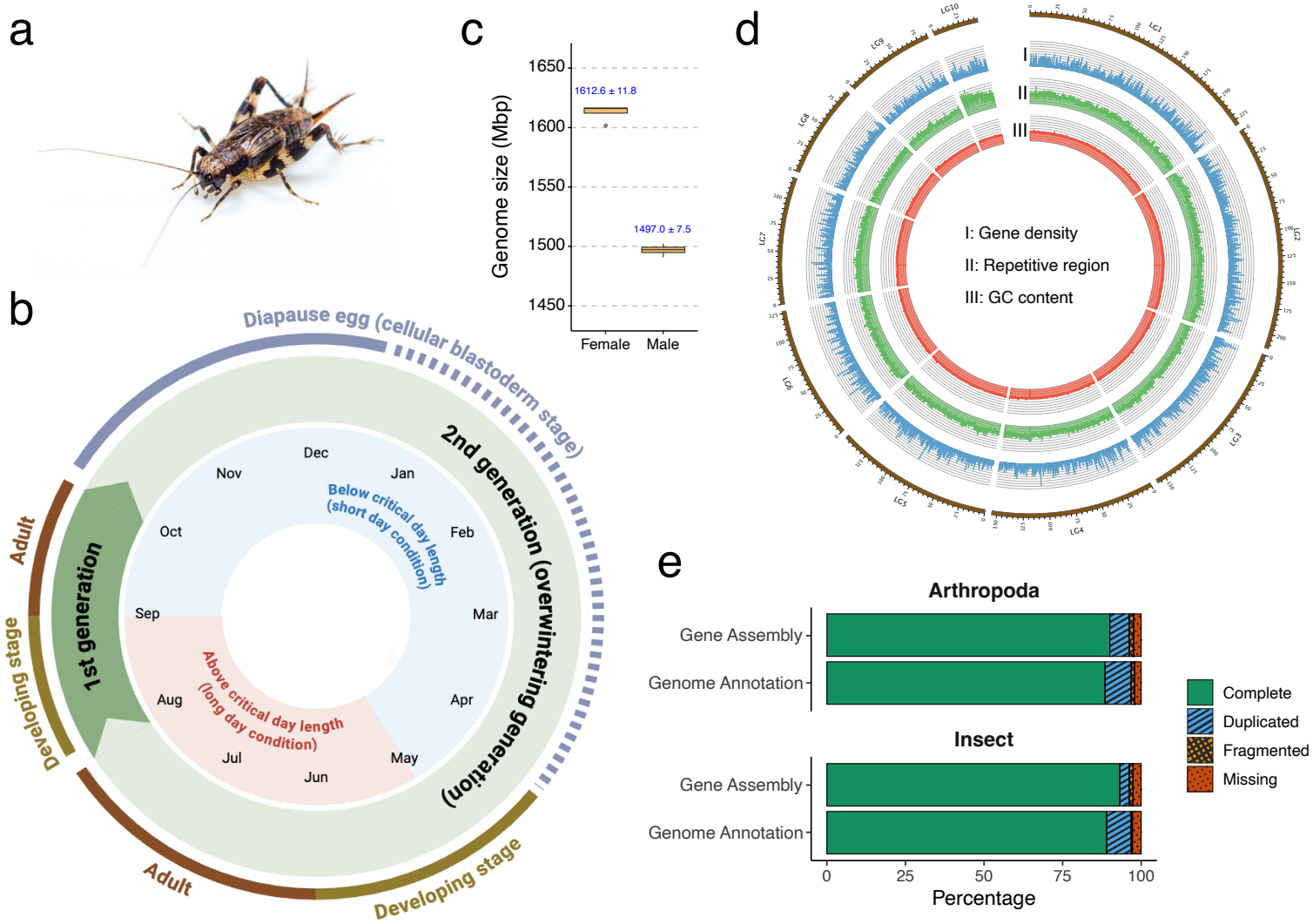
a
b
c
d
e
Genome size (Mbp)
1650
1600
1550
1500
1450
1612.6 ± 11.8
1497.0 ± 7.5
Female
Male
Diapause egg (cellular blastoderm stage)
2nd generation (overwintering generation)
1st generation
Adult
Developing stage
Adult
Developing stage
Dec
Jan
Feb
Mar
Apr
May
Jun
Jul
Aug
Sep
Oct
Nov
Below critical day length
(short day condition)
Above critical day length
(long day condition)
I
II
III
I: Gene density
II: Repetitive region
III: GC content
Arthropoda
Insect
Gene Assembly
Genome Annotation
Complete
Duplicated
Fragmented
Missing
0
25
50
75
100
Percentage

Figure 2

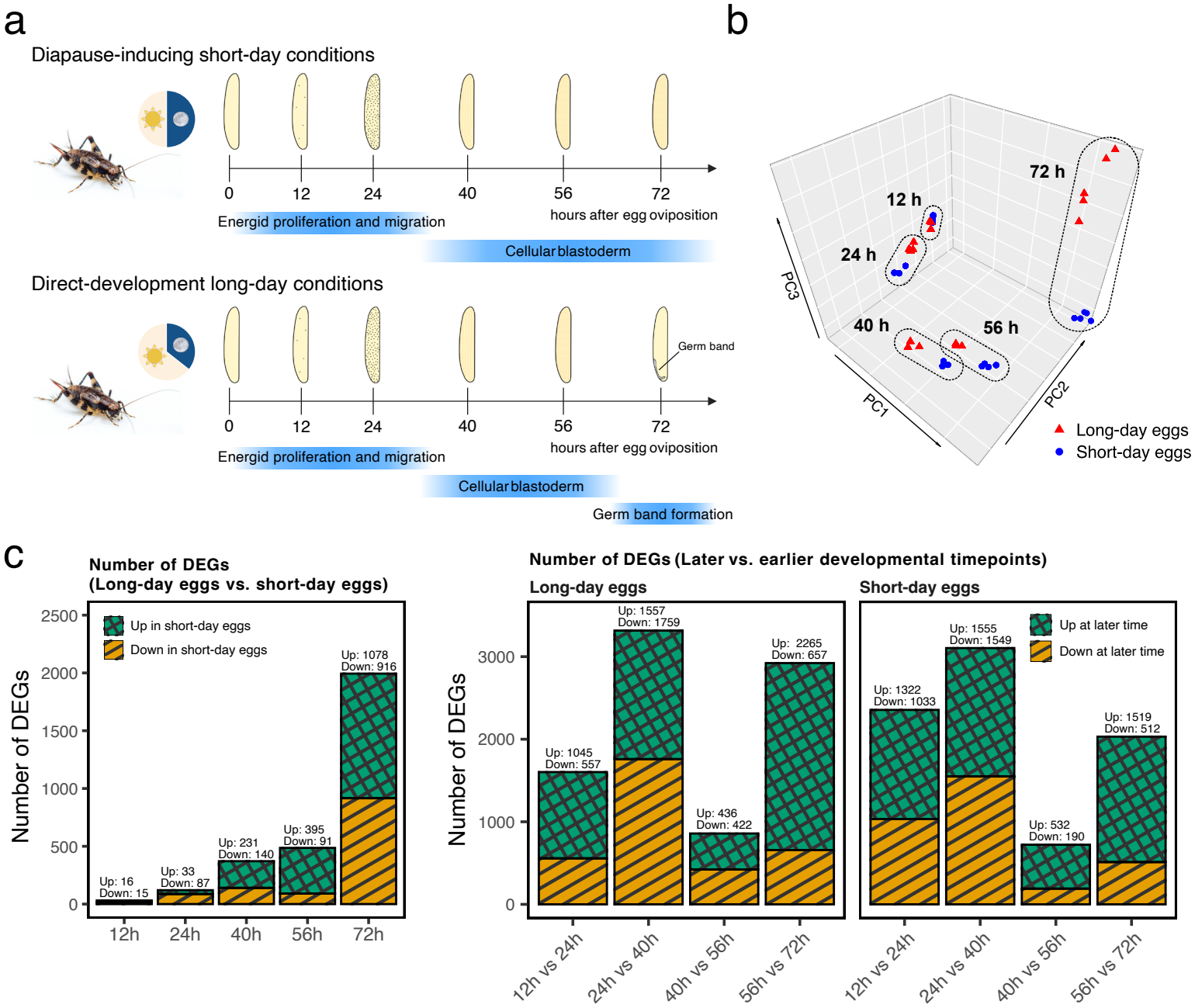
a
Diapause-inducing short-day conditions
0
12
24
40
56
72
hours after egg oviposition
Energid proliferation and migration
Cellular blastoderm
Direct-development long-day conditions
Germ band
Germ band formation
b
12 h
24 h
40 h
56 h
72 h
PC1
PC2
PC3
Long-day eggs
Short-day eggs
c
Number of DEGs
(Long-day eggs vs. short-day eggs)
Up in short-day eggs
Down in short-day eggs
Number of DEGs
Up: 16
Down: 15
Up: 33
Down: 87
Up: 231
Down: 140
Up: 395
Down: 91
Up: 1078
Down: 916
12h
24h
40h
56h
72h
Number of DEGs (Later vs. earlier developmental timepoints)
Long-day eggs
Short-day eggs
Up at later time
Down at later time
Up: 1045
Down: 557
Up: 1557
Down: 1759
Up: 436
Down: 422
Up: 2265
Down: 657
Up: 1322
Down: 1033
Up: 1555
Down: 1549
Up: 532
Down: 190
Up: 1519
Down: 512
12h vs 24h
24h vs 40h
40h vs 56h
56h vs 72h

Figure 3

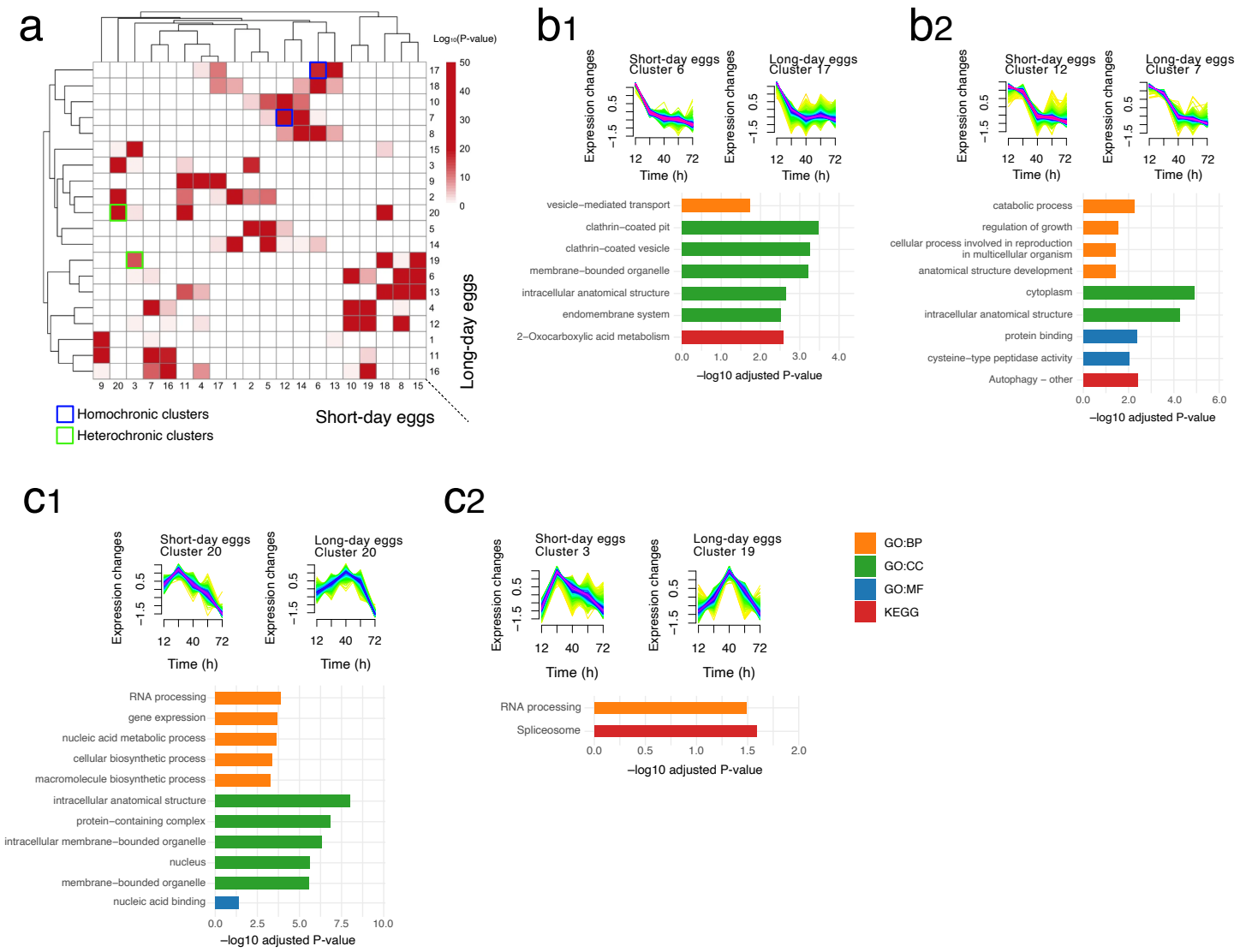
a
Log10(P-value)
Homochronic clusters
Heterochronic clusters
Short-day eggs
Long-day eggs
b1
Short-day eggs Cluster 6
Long-day eggs Cluster 17
Expression changes
Time (h)
vesicle−mediated transport
clathrin−coated pit
clathrin−coated vesicle
membrane−bounded organelle
intracellular anatomical structure
endomembrane system
2−Oxocarboxylic acid metabolism
−log10 adjusted P-value
b2
Short-day eggs Cluster 12
Long-day eggs Cluster 7
catabolic process
regulation of growth
cellular process involved in reproduction in multicellular organism
anatomical structure development
cytoplasm
intracellular anatomical structure
protein binding
cysteine−type peptidase activity
Autophagy − other
C1
Short-day eggs Cluster 20
Long-day eggs Cluster 20
RNA processing
gene expression
nucleic acid metabolic process
cellular biosynthetic process
macromolecule biosynthetic process
intracellular anatomical structure
protein−containing complex
intracellular membrane−bounded organelle
nucleus
membrane−bounded organelle
nucleic acid binding
C2
Short-day eggs Cluster 3
Long-day eggs Cluster 19
RNA processing
Spliceosome
GO:BP
GO:CC
GO:MF
KEGG

Figure 4

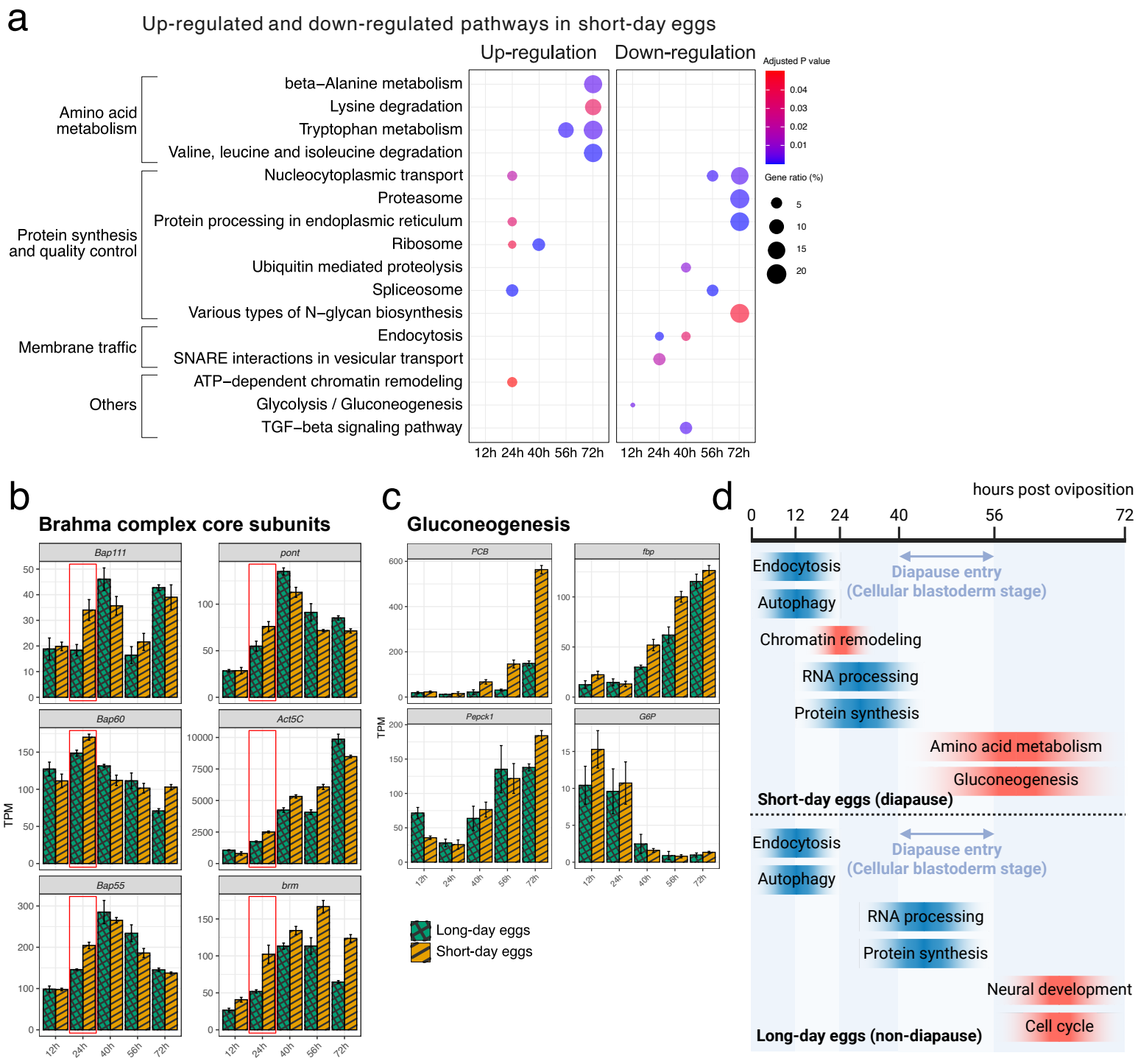
a
Up-regulated and down-regulated pathways in short-day eggs
Up-regulation
Down-regulation
Adjusted P value
0.04
0.03
0.02
0.01
Gene ratio (%)
5
10
15
20
Amino acid metabolism
beta−Alanine metabolism
Lysine degradation
Tryptophan metabolism
Valine, leucine and isoleucine degradation
Protein synthesis and quality control
Nucleocytoplasmic transport
Proteasome
Protein processing in endoplasmic reticulum
Ribosome
Ubiquitin mediated proteolysis
Spliceosome
Various types of N−glycan biosynthesis
Membrane traffic
Endocytosis
SNARE interactions in vesicular transport
Others
ATP−dependent chromatin remodeling
Glycolysis / Gluconeogenesis
TGF−beta signaling pathway
12h 24h 40h 56h 72h
b
Brahma complex core subunits
Bap111
pont
Bap60
Act5C
Bap55
brm
TPM
c
Gluconeogenesis
PCB
fbp
Pepck1
G6P
Long-day eggs
Short-day eggs
d
hours post oviposition
0 12 24 40 56 72
Endocytosis
Autophagy
Diapause entry
(Cellular blastoderm stage)
Chromatin remodeling
RNA processing
Protein synthesis
Amino acid metabolism
Gluconeogenesis
Short-day eggs (diapause)
Endocytosis
Autophagy
Diapause entry
(Cellular blastoderm stage)
RNA processing
Protein synthesis
Neural development
Cell cycle
Long-day eggs (non-diapause)